ANGPLT3 Impacts Proteinuria and Hyperlipidemia in Primary Nephrotic Syndrome

Fu Zhong
Guangzhou Women and Children's Medical Center
Shurao Liu
The First People's Hospital of Zhaoqing
Yue Li
Guangzhou Women and Children's Medical Center
Jingzhi Wang
Guangzhou Women and Children's Medical Center
Weijing Cui
Gansu Provincial Hospital
Yanhong Suo
Gansu Provincial Hospital
Xia Gao (gaoxiagz@vip.163.com)
Guangzhou Women and Children's Medical Center https://orcid.org/0000-0003-4412-5166

Research Article

Keywords: ANGPTL3, hyperlipidemia, proteinuria, nephrotic syndrome

Posted Date: October 28th, 2021

DOI: https://doi.org/10.21203/rs.3.rs-1012651/v1

Abstract

Background: It is unclear why primary nephrotic syndrome (PNS) patients often have dyslipidemia. Recent studies have shown that angiopoietin-like protein 3 (ANGPTL3) is an important regulator of lipid metabolism. In this study, we explored how ANGPTL3 impacts dyslipidemia in PNS development.

Methods: We measured the serum levels of ANGPTL3 in PNS patients. Furthermore, the degree of proteinuria and lipid metabolism were examined in *angptl3*-overexpressing transgenic (*angptl3*-tg) mice at different weeks of age. Moreover, this study used the clustered regularly interspaced short palindromic repeats-associated protein 9 (CRISPR/Cas9) system to create *angptl3*-knockout (*angptl3*-/-) mice to observe lipopolysaccharide (LPS)-induced nephrotic mice.

Results: There was a significant correlation between the serum level of ANGPTL3 and the levels of cholesterol, triglycerides and low-density lipoprotein in PNS patients. With increasing age, *angptl3*-tg mice exhibited increasingly severe hypertriglyceridemia and proteinuria. The pathological features included rich lipid droplet deposition in hepatocytes and diffuse podocyte effacement in *angptl3*-tg mice. Compared to wild-type mice, *angptl3*-/- mice showed significantly lower degrees of lipid dysfunction and proteinuria after stimulation with LPS. The effects of ANGPTL3 on nephrotic dyslipidemia were confirmed in cultured hepatocytes with *angptl3* knockdown or overexpression. Finally, significant alterations in lipoprotein lipase (LPL) were observed in liver tissues from Angptl3-/- and wild-type mice stimulated with LPS.

Conclusion: ANGPTL3 could be involved in the development of dyslipidemia, as well as proteinuria, in PNS pathogenesis. Inhibiting LPL expression may be why ANGPTL3 induces hyperlipidemia in PNS.

Introduction

Proteinuria and hyperlipidemia are considered to be the most important clinical features of primary nephrotic syndrome (PNS). Among them, proteinuria is the core characteristic of PNS. Podocyte injury in the outermost layer of the glomerular filtration barrier plays a key role in the development of PNS proteinuria[1]. Hyperlipidemia is another important feature of PNS, which often appears during the acute phase and disappears in the remission phase of the disease. Abnormal lipoprotein lipase (LPL) activity is considered to be one of the mechanisms leading to PNS hyperlipidemia[2]. However, why PNS results in massive proteinuria and hyperlipidemia at the same time and whether these two pathophysiological phenomena have a common pathogenesis are questions of interest.

Angiopoietin-like protein 3 (ANGPTL3) belongs to the angiopoietin-like protein family. ANGPTL3 is mainly synthesized by liver cells and is notably expressed in kidney podocytes[3]. Recently, a series of experiments showed that ANGPTL3 could induce cytoskeletal rearrangement in podocytes, leading to increased podocyte motility[4]. Some studies have revealed that ANGPTL3 is involved in the development

of nephrotic proteinuria by attenuating podocyte foot effacement and podocyte detachment from glomeruli[5].

As a lipid regulating reagent, ANGPTL3 has been extensively studied with respect to lipid metabolism[6]. ANGPTL3 can significantly inhibit the activity of LPL, leading to reduced triglyceride and cholesterol decomposition and increased blood lipids, and is a key molecule that regulates lipid metabolism[7]. And recent reported study about ANGPTL3 plasma levels and extra-coronary arterial health showed that the ankle–brachial blood pressure index was significantly associated with ANGPTL3 levels[8].

In this study, we examined whether ANGPTL3 could regulate lipid metabolism in vivo or in vitro in PNS models, and using *angptl3*-tg mice, we examined the multiple effects of ANGPTL3. Finally, we explored the role of LPL in the mechanism of ANGPTL3 in PNS hyperlipidemia.

Methods

Antibodies and reagents

The antibodies and reagents used in this study are listed with their sources in parentheses as follows: monoclonal antibodies against glyceraldehyde-phosphate dehydrogenase (GAPDH) (ImmunoWay Biotechnology, Texas, USA), polyclonal antibodies against ANGPTL3 (R&D Systems, Minneapolis, USA), and polyclonal antibodies against LPL (Santa Cruz Biotechnology, Santa Cruz, CA). Lipopolysaccharide (LPS) was purchased from Pfizer Inc., USA.

Production of Cas9 mRNA and sgRNA

The T7 promoter was added to the Cas9 coding sequence by polymerase chain reaction (PCR) amplification using the PX330 vector (Addgene) and the primer Cas9 (F and R) (**Table S1**). The T7-Cas9 PCR product was gel purified by a QIAquick Gel Extraction Kit (Qiagen, USA) and used as the template (500 ng) for in vitro transcription (IVT) using the mMESSAGEmMACHINE T7 ULTRA Transcription Kit (Thermo Fisher Scientific, USA). Both the T7 promoter and targeting sequence were added to sgRNA by PCR amplification using the primer sgAngptl3 (F and R) (**Table S1**). The T7-sgRNA PCR product was also purified on gels using a QIAquick Gel Extraction Kit (Qiagen, USA) and then used as a template (250 ng) for IVT using a MEGA short script T7 kit (Thermo Fisher Scientific, USA). Both Cas9 mRNA and sgRNA were purified according to the standard protocol by phenol:chloroform extraction and ethanol precipitation and were then dissolved in DNase/RNase-free water (Thermo Fisher Scientific, USA).

Generation of Angptl3-knockout mice

Female C57BL/6 mice (6–8 weeks old) were used as embryo donors. Female C57BL/6 mice were superovulated by intraperitoneal injection with pregnant mare serum gonadotropin (PMSG) and human chorionic gonadotropin (hCG) and then mated with male C57BL/6 mice. Fertilized embryos (zygotes)

were collected from the oviducts. Cas9 mRNA (100 ng/μL) and sgRNA (*angptl3*) (50 ng/μL) were mixed and injected into the cytoplasm of fertilized eggs with both pronuclei visible in CZB (Chatot–Ziomek–Bavister) medium. The injected zygotes were then cultured in Quinn's Advantage cleavage medium (In Vitro Fertilization, Inc.) at 37 °C and 5% CO_2 for approximately 24 h, and 18–20 2-cell stage embryos were transferred into the oviduct of a pseudopregnant ICR female mouse at 0.5 dpc. This work was performed at Shanghai Gemple Biotech Co. Ltd.

Mouse identification and maintenance

Angptl3-/- mice were generated by the clustered regularly interspaced short palindromic repeats-associated protein 9 (CRISPR/Cas9) system. All mice had access to food and water. All experiments were performed in accordance with the Health Guide for the Care and Use of Laboratory Animals and were approved by the Biological Research Ethics Committee of Gansu Province People's Hospital (No. syll20130331). Genotyping of *angptl3*-/- mice was performed by PCR analysis of mouse tail-tip genomic DNA using *angptl3* primers (F and R) (**Table S2**) and then analyzed by Sanger sequencing. This work was performed in the Animal Center of Gansu University of Traditional Chinese Medicine. All mice were housed in an air-conditioned room and were provided free access to food and water (22 ± 2 °C; 12:12-hour light:dark cycle). After the mice were anesthetized with 10% chloral hydrate (400 mg/kg), the mice were euthanized by cervical dislocation, and all efforts were undertaken to minimize pain and discomfort. The mice did not exhibit signs of peritonitis after the administration of 10% chloral hydrate (400 mg/kg).

Generation of *angptl3*-knockout mice

The double-strand breaks (DSBs) induced by the CRISPR/Cas9 system stimulate DNA repair by at least two distinct mechanisms, nonhomologous end joining (NHEJ) and homology-directed repair (HDR). NHEJ is error-prone and introduces unpredictable patterns of insertions and deletions (Indel), which can lead to disruptions in the protein-coding capacity of a defined locus. To generate *angptl3*-knockout mice, we injected Cas9 mRNA and sgRNA targeting *angptl3* exon 1, which contains the start codon, into fertilized eggs (**Fig. S1a**). Subsequent subcloning of the flanking regions surrounding the sgRNA targeting site identified four founder mice with frameshift mutations (**Fig. S1b**).

Generation of *angptl3* transgenic mice

Murine *angptl3* cDNA was synthesized by Shanghai Gemple Biotechnology and cloned into the pcDNA3.1 vector (**Fig. S2a**). This plasmid, designated pcDNA3.1-Angptl3, was linearized by MluI/DraIII, and the fragment of interest was then purified for oocyte injection into C57Bl/6 mouse-derived fertilized eggs[9-10]. Transgenic mice were identified by PCR using oligonucleotide primers specific for the construct (CMV-F, 5'-CGCGTTGACATTGATTATTGA CTA -3' and *angptl3*-R, 5'- CAGGAGGCCATTCG CTAAAA -3'; PCR fragment =892 bp) (**Fig. S2b**).

Generation of LPS nephrosis in mice

All animal studies were approved by the Subcommittee on Research Animal Care of the Gansu Province People's Hospital (No. syll20130331) and performed in the Animal Center of Gansu University of Traditional Chinese Medicine. Thirty-six male wild-type or Angptl3-/- C57BL/6 mice 6- to 8-weeks old were given free access to standard laboratory food and water. Both groups of mice were injected intraperitoneally with 200 μg of LPS (1 mg/ml in sterile LPS-free PBS) in a total volume of 200 μl. Mice in the control group (n 5) were intravenously administered an identical volume of saline. After the four groups were injected, urinary protein excretion was measured at 24 hours, 48 hours, and 72 hours, and kidney and liver tissues were harvested and processed for H&E staining. FP effacement was assessed by transmission electron microscopy according to our published protocols[11]. After LPS injection, the mice were killed at 24 h, 48 h, and 72 h, during which time no unexpected deaths were observed. The humane endpoint was defined as weight loss of 20%, dyspnea, or difficulty feeding within 72 hours of LPS injection. Death was confirmed by the absence of a pulse, breathing, corneal reflex, response to toe pinch and a lack of respiratory sounds and heartbeat.

Objectives

In this study, 196 patients with PNS who were admitted to Gansu Province People's Hospital from Jan 2016 to Jan 2018 from china were enrolled, including 124 males and 72 females. The study protocol conformed to the ethical guidelines of the 2013 Declaration of Helsinki. We ensured that all patients and healthy controls provided informed and written consent for the study, and ethics approval was obtained from the Gansu Province People's Hospital Research Ethics Committee (syll 20160037).

PNS met the inclusion criteria of nephrotic syndrome, with urinary protein > 3.5 g/d and plasma albumin < 30 g/L, accompanied by varying degrees of edema and/or hyperlipidemia[12-13]. The exclusion criteria were as follows: PNS patients without the required clinical and laboratory data, those with secondary nephrotic syndrome, a previous history of other acute or any stage of chronic kidney disease, patients with abnormal ultrasound examination of the urinary system (e.g., deformities, cysts, hydrops, stones), acute or chronic illness (diabetes mellitus, thyroid dysfunction, polycystic ovary syndrome, obesity, fatty liver, familial hypercholesterolemia), and other systemic diseases, such as hematological diseases, cardiovascular diseases, connective tissue diseases, tumors, and obvious infections.

There were 196 patients with PNS included in this study, including 72 females (36.54%) and 124 males (63.46%), with a male-to-female ratio of 1:0.58. The average age of the PNS group was 32(32.88-37.75) and that of the healthy control group was 31.5(29.37-42.83), and there was no significant difference between the two groups ($P > 0.05$), as shown in **Table 1**.

Experimental methods

(1) Sample collection: Elbow venous blood (3 ml) was collected from fasting subjects in the morning in an anticoagulant test tube. Serum was separated after centrifugation for 5 minutes (800 x g) and transferred to EP tubes. Five milliliters of urine was collected and placed in a test tube without any

additives. After being centrifuged for 5 minutes (800 x g), the supernatant was collected and transferred into EP tubes. Serum and urine were frozen at -80 °C for use.

1. Detection of serum and urine biochemical indicators: Biochemical indicators such as triglyceride (TG), total cholesterol (TC), high density lipoprotein (HDL-C), low density lipoprotein (LDL-C), serum creatinine (Scr), urea nitrogen (BUN), and 24-hour urea protein (24 hUP) were measured by an automatic biochemical analyzer (ABBOTT ARCHITECT c1600, USA).
2. Determination of ANGPTL3 levels in serum: The concentration of ANGPTL3 in serum was measured by ELISA kits for human ANGPTL3, and the specific protocol was carried out strictly according to the instructions.

Hepatocyte cell line culture and treatment

A nontumorigenic mouse hepatocyte cell line (AML12) was obtained from the American Type Culture Collection (ATCC) and cultured in DMEM/F12 medium (Gibco) containing 5 μg/ml ITS premix (Sigma–Aldrich, USA), 40 ng/ml dexamethasone (Sigma–Aldrich), and 10% fetal bovine serum (FBS, Gibco) at 37 °C in a humidified atmosphere with 5% CO2. Lipopolysaccharide (LPS; working concentration: 25 μg/ml) was purchased from Sigma–Aldrich. AML12 cells were collected after LPS stimulation for 24 h.

Lentiviral infection

To produce ANGPTL3 overexpression or knockdown lentivirus, the lentivirus with the murine angptl3 coding sequence or angptl3 shRNA and blank control were purchased from Gemple Biotechnology (Shanghai, China). The target sequences of angptl3 shRNA were as follows: sh angptl3#1, 5′-GCTGGG TCATGGACTTAAAG-3′; and sh angptl3#2, 5′-GCAGCTAACCAACTTAA TTC-3′. AML12 cells were infected with recombinant lentivirus plus 8 μg/ml polybrene (Sigma–Aldrich) at a multiplicity of infection (MOI) of 20. Stable lentivirus-infected cells were selected and enriched by flow cytometry (BD).

RNA extraction and quantitative RT–PCR

Total RNA was extracted using a Direct-zol RNA MiniPrep kit (Zymo Research, USA) according to the manufacturer's instructions. Total mRNA (1 μg) was reverse transcribed using 5X All-In-One RT MasterMix (Abm, Canada) according to the manufacturer's instructions. Real-time PCR (**RT–PCR**) was performed using SYBR FAST qPCR Kit Master Mix (2X) Universal (KAPA, USA) on an Applied Biosystems 7,500 Fast RT–PCR System (Foster City, USA). The RT–PCR system involved cDNA (1.0 μl), 2X SYBR-Green Mix (10 μl), forward primer (10 μM, 0.5 μl), reverse primer (10 μM, 0.5 μl), and RNase-free water in a final volume of 20 μl. The reaction conditions were as follows: 2 min of denaturation at 94 °C, 40 cycles of 1 min at 94 °C, 30 sec at 56 °C, 2 min at 72 °C, and a final extension step at 72 °C for 10 min. The cycle threshold (Ct) values were analyzed using the comparative Ct (ΔΔCt) method according to the MIQE guidelines. The amount of the target was normalized to an endogenous reference (GAPDH) and is expressed relative to the control (nontreated cells). The primers used were as follows: ANGPTL3 (forward, 5′-

GCGAACATACAAGTGGCGTG-3’; reverse, 5’-CTGTGAGCCATCT TTCCGGT-3’); and LPL (forward, 5’-GAAAACCCCAGC AAGGCATAC -3’; reverse, 5’- CATCTTGCTGCTTCTCTTGGC -3’).

Oil Red O Staining

Oil Red O staining was performed with an Oil Red O Stain Kit (Jiancheng Bioengineering Institute, Nanjing, China) according to the manufacturer's instructions. The results were examined by a light microscope, and the OD560 was measured for quantification.

Western blotting

We performed immunoblotting experiments as described previously[4].

Statistical analysis

The experimental data were tested for normality using the Kolmogorov–Smirnov method, and the chi-square test was performed using Levene's test for variance equations. All quantitative information conforming to a normal distribution is expressed as x±s and was analyzed using independent sample t tests; nonnormally distributed quantitative data are expressed as median and95%CI and were analyzed using the Mann–Whitney U test; and the difference in the sex ratios were tested by the X^2 test. Pearson correlation analysis was used to examine correlations between variables of two measures that obeyed normal distribution; the Spearman rank correlation test was used to analyze correlations between variables of two measures that did not obey normal distribution. The values from animals or cells were subjected to one-way ANOVA, and Pearson correlations among the groups were calculated. *P* values of <0.05 were considered statistically significant. The data were statistically processed using SPSS 20.0 software.

Results

The serum level of ANGPTL3 correlated with blood lipids in PNS patients.

In this study, we analyzed the serum level of ANGPTL3. Compared with that in the healthy group, the serum level of ANGPTL3 in the PNS group was significantly increased (32(26.35-39.66) ng/ml vs. 70.44(63.95-76.51) ng/ml, Z =-4.81, $P < 0.001$). Furthermore, we analyzed the correlation between serum ANGPTL3 levels and major indicators of blood lipids and found that ANGPTL3 positively correlated with CHO to a low degree (r=0.34, $P < 0.001$), with TGs to a low degree (r= 0.25, $P = 0.001$), and with LDL-C to a moderate degree (r= 0.50, $P < 0.001$), but there was no correlation with HDL-C (**Table 2**, r= 0.15, $P = 0.07$).

Under physiological conditions, lipid levels and proteinuria in *angptl3*-knockout C57 mice were nearly normal

We observed laboratory indications and pathological features of *angptl3*-/- mice under physiological conditions. There was no significant difference in the serum TG or TC between wild-type mice and

angptl3-/- mice (**Fig. 1a, b** $P > 0.05$). The 24 h urine protein results showed that there was no difference between *angptl3*-/- mice and wild-type mice (**Fig. 1c**, $P > 0.05$). The liver structure of *angptl3*-/- mice was observed under a light microscope, and there was no difference between wild-type and *angptl3*-/- mice. No inflammatory cell infiltration was observed (**Fig. 1d**). The glomerular structure of knockout mice was also normal under a light microscope and electron microscope (**Fig. 1e, f**).

In an LPS nephrotic mouse model, *angptl3* knockout in C57 mice alleviated proteinuria or hyperlipidemia

To explore whether ANGPLT3 impacts dyslipidemia under PNS conditions, we compared changes in the main indices of blood lipids in wild-type and *angptl3*-/- mice after LPS induction. As shown in **Fig. 2a** and **b**, compared with those in the WT group, mice in the WT+LPS group developed significant hypertriglyceridemia and hypercholesterolemia after 48 hours ($P < 0.05$). The TG and TC levels in the *angptl3*-/-+LPS group were lower than those in the WT+LPS group at 24 h and 48 h, and a significant difference was observed at 72 h ($P < 0.05$).

Then, we observed lipid droplet deposition in the liver tissues in each group of mice at 72 h. The results showed liver cell vacuolar degeneration in the WT+LPS group compared with the WT group, indicating that lipid droplets accumulated in large amounts in hepatocytes (**Fig. 2d)**. In contrast to that of wild-type mice, lipid droplet deposition in the liver tissues of *angptl3*-/- mice showed a significantly reduced trend after LPS stimulation.

In this study, we also compared the changes in proteinuria in *angptl3*-/- mice and wild-type mice in an LPS nephropathy model. As shown in **Fig. 2c**, at 24, 48 and 72 hours after LPS induction, the proteinuria levels of *angptl3*-/- mice at the different time points were significantly lower than those of wild-type mice ($P < 0.05$).

The structure of glomeruli and podocytes was observed and was consistent with the pathological phenotype of MCD, and the structure of glomeruli in wild-type mice after LPS stimulation was mainly normal under a light microscope. The podocytes of LPS nephropathy mice were extensively fused under an electron microscope. However, the degree of podocyte fusion in *angptl3*-/- mice was significantly lower than that in wild-type mice after LPS stimulation (**Fig. 2e)**.

Transgenic *angptl3* mice developed hyperlipidemia accompanied by proteinuria

To verify whether ANGPTL3 is involved in both lipid metabolism and proteinuria, angptl3-transgenic mice were examined. As shown in **Fig. 3a, b**, the triglycerides and total cholesterol levels of *angptl3*-tg mice were significantly higher than those of wild-type mice at the three time points ($P < 0.01$), and the serum lipid index of angptl3-tg mice gradually increased beginning 6 weeks after birth. Furthermore, we compared possible differences in the degree of dyslipidemia between the LPS nephrotic model and *angptl3*-tg mice. Wild-type mice at 6, 24 and 36 weeks of age were stimulated with LPS. The triglyceride and total cholesterol levels in LPS-stimulated mice were measured after 72 hours of LPS stimulation. Furthermore, the triglycerides of *angptl3*-tg mice were significantly lower than those of LPS mice at the

same age (**Fig. 3a,** P <0.01). In contrast to the triglyceride level, the total cholesterol level was not obviously different between *angptl3*-tg mice and the LPS model mice at each age.

In addition, compared with those of wild-type mice, the 24-hour proteinuria quantification results suggested that the *angptl3*-tg mouse proteinuria levels increased significantly at week 6 (**Fig. 3c,** P < 0.01). After week 24, the increasing trend was decreased, but the level of proteinuria was still significantly higher than that of wild-type mice of the same age (P < 0.05). The 24-hour proteinuria level in the *angptl3*-tg group was always significantly lower than that in the wild-type group after modeling (P < 0.01) at each time point. In addition, podocyte injury in *angptl3*-tg mice was observed by electronic microscopy, and the results showed that podocyte foot effacement became increasingly diffuse with age **(Fig. 3d)**.

ANGPTL3 regulated lipid metabolism in nephrotic hepatocytes *in vitro*.

In this study, lipid metabolism in nephrotic hepatocytes was observed by oil red staining. The results showed that the staining area of wild-type hepatocytes stimulated with LPS was significantly increased compared with that of the untreated group (**Fig. 4a, b**). The oil red staining area in hepatocytes overexpressing ANGPTL3 was enlarged (**Fig. 4a, b**). The area of lipid droplets in ANGPTL3-knockdown hepatocytes was significantly smaller than that of wild-type hepatocytes, and both cell lines were stimulated with LPS (**Fig. 4a, b**).

The TG and LDL levels in each group were further measured by ELISA, as shown in **Fig. 4c, d**. Wild-type and ANGPTL3-knockdown hepatocytes were stimulated with LPS. We found that the levels of TG and LDL in the miRNA+LPS group were significantly lower than those in the WT+LPS group. TG and LDL levels in Teg podocytes overexpressing ANGPTL3 were both higher than those in the WT group.

ANGPTL3 affected the occurrence of PNS hyperlipidemia by affecting LPL

In this study, we measured the expression of ANGPLT3 in liver tissue and found that the mRNA and protein expression levels of ANGPTL3 in the livers of wild-type mice were significantly enhanced 24 h after LPS stimulation **(Fig. 5a, b**, **c**, P < 0.01). ANGPTL3 robustly inhibits the activity of LPL, which is an important factor associated with triglycerides and cholesterol metabolism. Real-time PCR and Western blotting were used to measure the mRNA and protein expression levels of LPL in the liver tissues of mice were stimulated with LPS for 24 h, 48 h and 72 h. The data showed that the mRNA and protein expression levels of LPL in the WT+LPS mice were significantly lower than those in the WT group at each time point (**Fig. 5d, e, f,** P < 0.05). However, the expression level of LPL in the Angptl3-/-+LPS group was significantly higher than that in the WT+LPS group (**Fig. 5e**, **f**, P < 0.05).

Discussion

The mechanism of the massive proteinuria and hyperlipidemia in primary nephrotic syndrome has not been clearly explained. Over the past 10 years, a large number of important signaling molecules and

mechanisms related to proteinuria have been identified in the context of podocyte injury[14-16], but the mechanism of PNS complicated with hyperlipidemia has been rarely reported.

As a member of the angiopoietin-like protein family, ANGPTL3 is well known as a powerful regulator of lipid metabolism that inhibits LPL function. There have been very few studies about this factor in PNS dyslipidemia. Recently, increasing evidence has suggested that ANGPTL3 is involved in the occurrence of nephropathy-associated proteinuria[4,11,17,18]. In our study, we explored the dual roles of ANGPTL3, which is involved not only in the occurrence of PNS proteinuria but also in hyperlipidemia. First, the data from PNS patients suggested that serum ANGPTL3 levels correlated with the degree of hyperlipidemia, as indicated by TG, CHO and LDL-C levels.

B6:129S5 genetic mice are naturally resistant to nephropathy[19], while C57BL/6 mice are known to be sensitive to the drugs that are commonly used to induce nephropathy[19-21]. Therefore, before establishing an animal model of nephropathy in this study, we first used CRISPR/Cas9 technology to knock out the *angptl3* gene in C57BL/6 mice and established *angptl3*-/- mice[10, 22]. Then, we examined the liver and kidney function and structural characteristics of *angptl3*-/- mice in the physiological state. We found that deletion of the *angptl3* gene did not affect kidney morphology or the glomerular and tubular structures of the mice, and no obvious structural abnormalities were observed in podocytes under an electron microscope. No obvious abnormalities in liver cells or bile duct structures in liver tissue were observed by light microscopy. Furthermore, there were no significant changes in serum lipid markers or urine protein levels in *angptl3*-/- mice compared with wild-type mice.

Further analysis of the characteristics of *angptl3* in the nephrotic model confirmed that the proteinuria level of *angptl3*-/- mice after LPS stimulation was significantly lower than that of wild-type mice. In accordance with our previous studies in B6:129S5 genetic mice, the podocytes in mice with *angptl3* gene knockout were slightly fused under an electron microscope, and the degree of podocyte fusion was significantly reduced compared with that of wild-type nephropathy mice[11].

Importantly, the hyperlipidemia levels of *angptl3*-/- mice after LPS stimulation were significantly lower than those of wild-type mice. Liver tissue analysis showed that liver cell vacuolization in *angptl3*-/- mice after LPS stimulation was significantly less than that of wild-type nephropathy mice. Additionally, in vitro data showed that hepatocytes transfected with *angptl3* also showed significantly enhanced oil red O staining. Compared with wild-type hepatocytes, *angptl3*-knockdown cells were less stained with oil red after LPS stimulation. Thus far, there has not been an ideal nephrotic animal model similar to human PNS. LPS-induced mice show transient nephrotic syndrome, and the pathology shows a minimal change disease (MCD). Therefore, our findings must be tested in additional nephrotic models, such as puromycin aminonucleoside (PAN)-

or adriamycin-induced focal segmental glomerulosclerosis (FSGS) models, which are widely used nephrotic models.

To demonstrate the role of ANGPTL3 in PNS hyperlipidemia, we also transfected C57 mice with *angptl3* and observed the changes in blood lipids and proteinuria in teg-angptl3 mice at different weeks of age. Our results demonstrated that high ANGPTL3 expression could lead to nephropathic manifestations with prolonged age, such as proteinuria, which suggests that ANGPTL3 participates in the development of both hyperlipidemia and proteinuria in mice. However, it is necessary to perform a longer observation to explore possible pathologic changes during the entire life in teg-angptl3 mice.

In this study, the alterations in LPL in liver tissue in wild-type or *angptl3*-/- mice with or without LPS stimulation suggested that ANGPTL3 markedly inhibited LPL expression in the PNS model. Our experiments showed that a large amount of ANGPTL3 was synthesized by hepatocytes in the context of nephropathy and participated in the occurrence of hyperlipidemia. In summary, the role of ANGPTL3 in regulating lipid metabolism, which was tested in this study, provides new insights regarding dyslipidemia in PNS. Based on the reported data, we think that some molecules, such as ANGPTL3, play multiple roles not only in proteinuria but also in hyperlipidemia. Our results may also provide new ideas for further study of the pathogenesis of PNS in the future.

Conclusion

ANGPTL3 could be involved in the development of dyslipidemia, in addition to proteinuria, in PNS pathogenesis. Inhibiting LPL expression may be the mechanism by which ANGPTL3 induces hyperlipidemia in PNS.

Abbreviations

PNS: primary nephrotic syndrome, ANGPTL3: angiopoietin-like protein 3, angptl3-tg: angptl3-overexpressing, angptl3-/-: angptl3-knockout, GAPDH: glyceraldehyde-phosphate dehydrogenase, DSBs: double-strand breaks, NHEJ: nonhomologous end joining, HDR: homology-directed repair., LPS: lipopolysaccharide, LXR: liver X receptors, LPL: lipoprotein lipase, TG: triglyceride, TC: total cholesterol, CHO: cholesterol, HDL: high density lipoprotein, LDL: low density lipoprotein, Scr: serum creatinine, BUN: urea nitrogen, 24 hUP: 24-hour urea protein, MCD: minimal-change disease. WT: wild-type mice, WL: wild-type mice treated with LPS, KN: Angptl3-/- mice, KL: Angptl3-/- mice stimulated with LPS. Teg: hepatocytes transfected Angptl3.

Declarations

Ethics approval and consent to participate

All patients and healthy controls agreed to participate in the study and signed informed consent forms. All experiments were performed in accordance with the Health Guide for the Care and Use of Laboratory Animals and were approved by the Biological Research Ethics Committee of Gansu Province People's Hospital (No. syll20130331).

Consent for publication

All authors read and approved this manuscript for publication.

Availability of data and materials

All data generated or analyzed during this study are included in this published article.

Competing interests

The authors declare that they have no competing interests.

Funding:

This work was supported by grants from the National Natural Science Foundation of China (Grant No. 81660130), the Natural Science Foundation of Gansu Province, China (Grant No. 18JR3RA045) and the Science and Technology Program of Guangzhou, China (Grant No. 202102010222).

Author's contributions

XG designed and directed the study and wrote the manuscript. FZ performed the majority of the experiments and analyzed the data. SL performed the animal experiments and analyzed the data. YL collected clinical samples and related data. JW participated in hepatocyte studies in vitro. WC examined the expression of LPL and ANGPTL3 in the different mouse groups. YS reviewed mouse kidney histopathology data and some Western blots.

Acknowledgments

We thank all of the staff in the Departments of Nephrology and Pediatric Hospital for their clinical assistance. We thank Yang Tong for his help with developing the Angptl3-/- and Angptl3-Tg mice. We express our appreciation to Zhigang Zhang for his help with electron microscopy.

References

1. Ding WY, Saleem MA. Current concepts of the podocyte in nephrotic syndrome. Kidney research and clinical practice. 2012;31(2):87-93.
2. Vaziri ND. Disorders of lipid metabolism in nephrotic syndrome: mechanisms and consequences. KIDNEY INT. 2016;90(1):41-52.
3. Koishi R, Ando Y, Ono M, Shimamura M, Yasumo H, Fujiwara T, et al. Angptl3 regulates lipid metabolism in mice. NAT GENET. 2002;30(2):151-7.
4. Gao X, Xu H, Liu H, Rao J, Li Y, Zha X. Angiopoietin-like protein 3 regulates the motility and permeability of podocytes by altering nephrin expression in vitro. BIOCHEM BIOPH RES CO. 2010;399(1):31-6.

5. Dai R, Liu H, Han X, Liu J, Zhai Y, Rao J, et al. Angiopoietin-like-3 knockout protects against glomerulosclerosis in murine adriamycin-induced nephropathy by attenuating podocyte loss. BMC NEPHROL. 2019;20(1):185.
6. Kersten S. Angiopoietin-like 3 in lipoprotein metabolism. Nature reviews. Endocrinology. 2017;13(12):731-9.
7. Minicocci I, Tikka A, Poggiogalle E, Metso J, Montali A, Ceci F, et al. Effects of angiopoietin-like protein 3 deficiency on postprandial lipid and lipoprotein metabolism. J LIPID RES. 2016;57(6):1097-107.
8. Liu J, Gao X, Zhai Y, Shen Q, Sun L, Feng C, et al. A novel role of angiopoietin-like-3 associated with podocyte injury. PEDIATR RES. 2015;77(6):732-9.
9. Eddy AA, Symons JM. Nephrotic syndrome in childhood. Lancet (London, England). 2003;362(9384):629-39.
10. Mahalingasivam V, Booth J, Sheaff M, Yaqoob M. Nephrotic syndrome in adults. Acute medicine. 2018;17(1):36-43.
11. Liu J, Afroza H, Rader DJ, Jin W. Angiopoietin-like protein 3 inhibits lipoprotein lipase activity through enhancing its cleavage by proprotein convertases. The Journal of biological chemistry. 2010;285(36):27561-70.
12. Dandapani SV, Sugimoto H, Matthews BD, Kolb RJ, Sinha S, Gerszten RE, et al. Alpha-actinin-4 is required for normal podocyte adhesion. The Journal of biological chemistry. 2007;282(1):467-77.
13. Michaud J, Lemieux LI, Dubé M, Vanderhyden BC, Robertson SJ, Kennedy CRJ. Focal and segmental glomerulosclerosis in mice with podocyte-specific expression of mutant alpha-actinin-4. Journal of the American Society of Nephrology : JASN. 2003;14(5):1200-11.
14. DeMali KA, Wennerberg K, Burridge K. Integrin signaling to the actin cytoskeleton. CURR OPIN CELL BIOL. 2003;15(5):572-82.
15. Rao J, Hong XU, Sun L, and Zhao ZH. Expression of ANGPTL3 in children with primary nephrotic syndrome. Chinese Journal of Nephrology. 2006;22(5):286-90.
16. Dai R, Lin Y, Liu H, Rao J, Zhai Y, Zha X, et al. A vital role for Angptl3 in the PAN-induced podocyte loss by affecting detachment and apoptosis in vitro. BMC NEPHROL. 2015;16:38.
17. Simic I, Tabatabaeifar M, Schaefer F. Animal models of nephrotic syndrome. Pediatric nephrology (Berlin, Germany). 2013;28(11):2079-88.
18. Srivastava T, Sharma M, Yew K, Sharma R, Duncan RS, Saleem MA, et al. LPS and PAN-induced podocyte injury in an in vitro model of minimal change disease: changes in TLR profile. J CELL COMMUN SIGNAL. 2013;7(1):49-60.
19. Reiser J, von Gersdorff G, Loos M, Oh J, Asanuma K, Giardino L, et al. Induction of B7-1 in podocytes is associated with nephrotic syndrome. The Journal of clinical investigation. 2004;113(10):1390-7.
20. Cong L, Ran FA, Cox D, Lin S, Barretto R, Habib N, et al. Multiplex genome engineering using CRISPR/Cas systems. Science (New York, N.Y.). 2013;339(6121):819-23.

21. Wu Y, Liang D, Wang Y, Bai M, Tang W, Bao S, et al. Correction of a genetic disease in mouse via use of CRISPR-Cas9. CELL STEM CELL. 2013;13(6):659-62.

Tables

Table 1 Comparison of basic charateristics between the both groups [($x \pm s$), n(%)]

	(n=60)	PNS(n=196)	t/x^2	*P*
Male /female	30/30	124/72	1.79	0.18
Ages(years)	36.10±14.378	35.32±14.348	-0.23	0.82
CHO (mmol/L)	3.70±0.932	7.01±2.862	10.30	<0.001
TG (mmol/L)	1.04±0.455	2.44±1.519	8.44	<0.001
LDL (mmol/L)	1.92±0.494	4.47±2.246	11.48	<0.001
HDL (mmol/L)	1.18±0.314	1.92±0.853	7.29	<0.001
24hUP(g/d)	0.09±0.019	3.12±5.063	6.98	<0.001
ALB(g/L)	43.85±6.062	31.60±9.162	-7.82	<0.001
Scr(umol/L)	50.11±17.730	84.30±57.858	2.63	0.01
BUN(mmol/L)	5.35±1.567	9.44±28.193	0.65	0.52
Serum ANGPTL3(ng/ml)	33.0114.226	70.2337.045	8.23	<0.001

Note: CHO cholesterol, TG triglyceride, LDL low density lipoprotein, HDL high density lipoprotein.

Table 2 The correlation between serum ANGPTl3 and lipid

Factor	Serum ANGPTL3	
	r/r_s	*P*
CHO	0.34	<0.001
TG	0.25	0.001
LDL	0.50	<0.001
HDL	0.15	0.07

Note: CHO cholesterol, TG triglyceride, LDL low density lipoprotein, HDL high density lipoprotein.

Figures

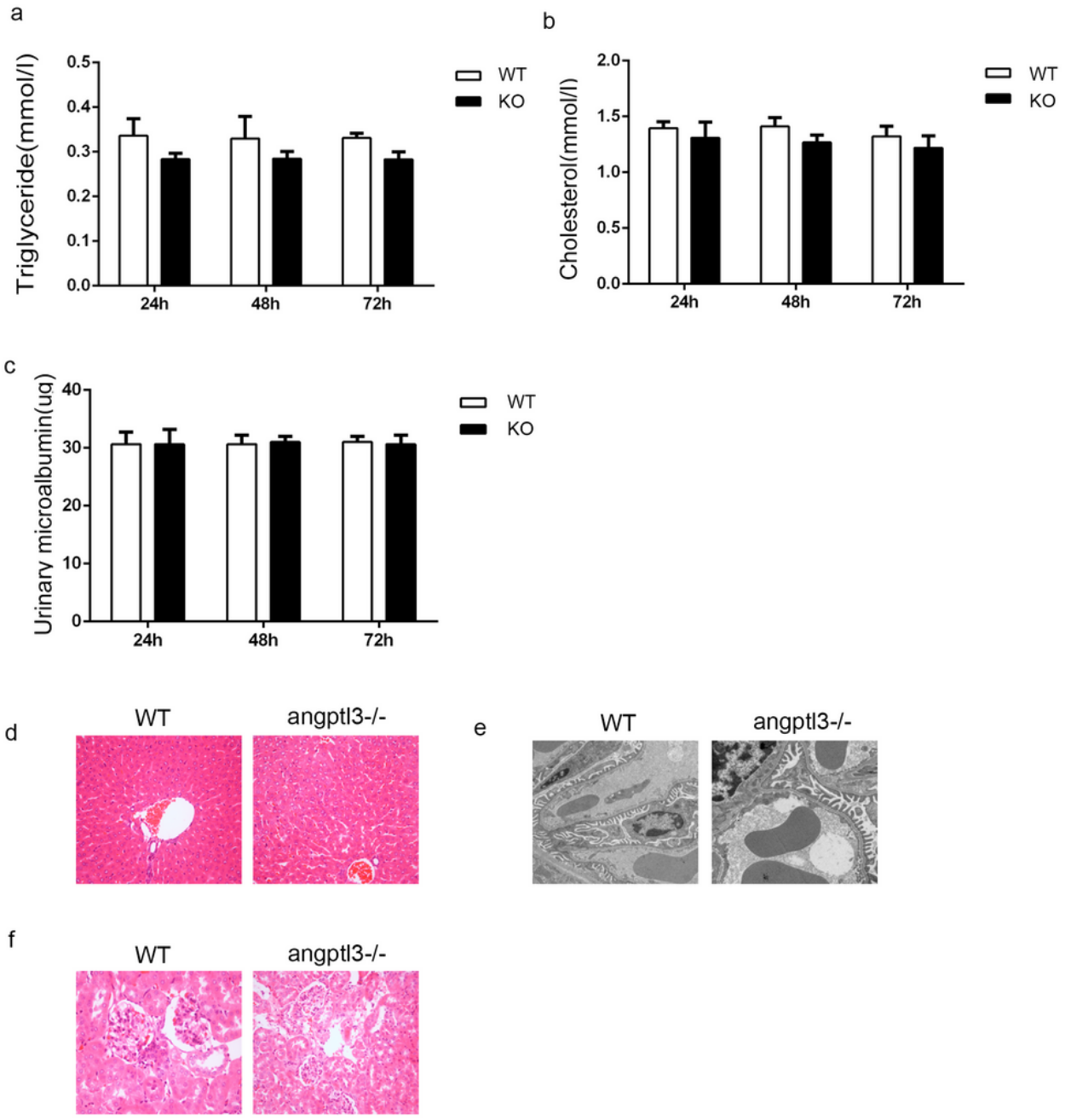

Figure 1

Under physiological conditions, lipid levels and proteinuria in angptl3-knockout C57 mice were nearly normal. a, b, c: The levels of triglycerides, cholesterolemia and proteinuria were not different between the groups. ($P > 0.05$). d: Under a light microscope, there were no changes in the liver structure between wild-type and angptl3-/- mice. e, f: The glomerular structure of knockout mice was also normal under a light

microscope and electron microscope. WT: wild type mice, KO: Angptl3-/- mice. *P<0.05 **P<0.01 the P values were subjected to independent-sample t tests.

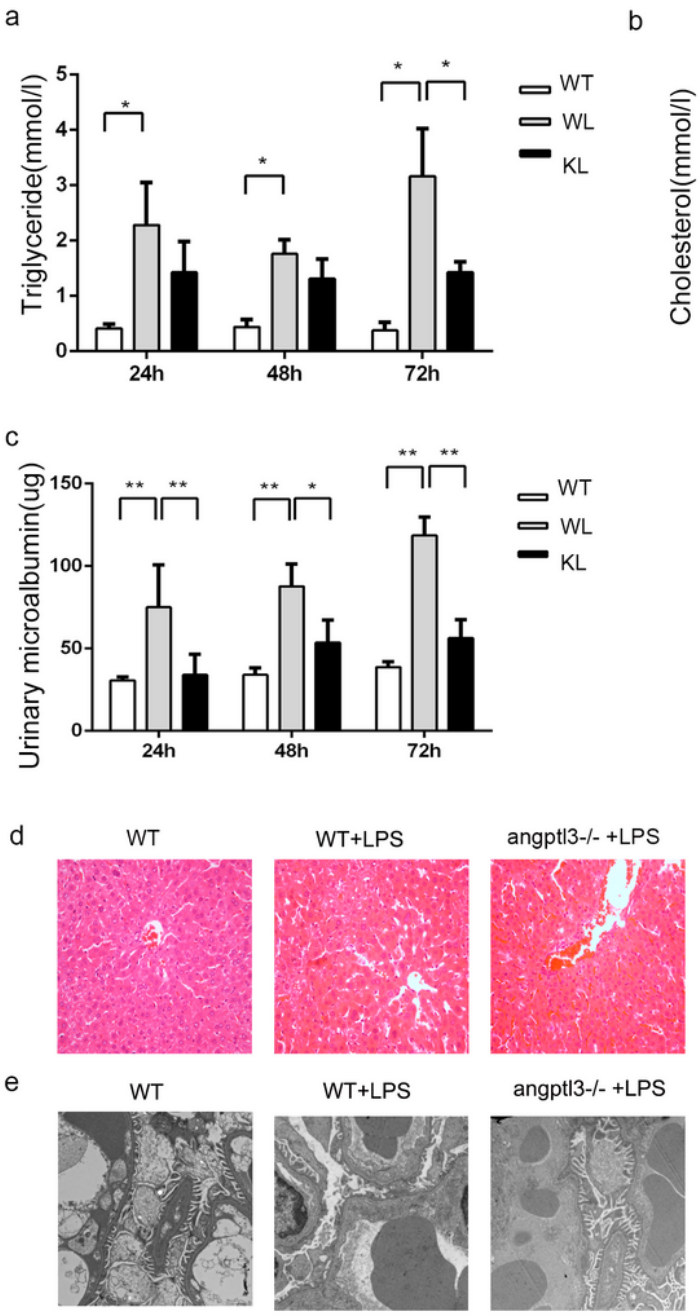

Figure 2

Knockout of the angptl3 gene did not affect the liver or kidney function of mice in the physiological state and played an important role in LPS-induced nephropathy. a, b, c: The levels of triglycerides, cholesterolemia and proteinuria in the three groups. d: Lipid droplet deposition in the liver tissue of each

group of mice, and the magnification is 400 X. e: Changes in the different groups, and the magnification is 5,000 X. WT: wild-type mice, WL: wild-type mice stimulate with LPS, KL: Angptl3-/- mice stimulated with LPS. Each group included 5 mice. *P<0.05 **P<0.01 the P values were subjected to one-way ANOVA.

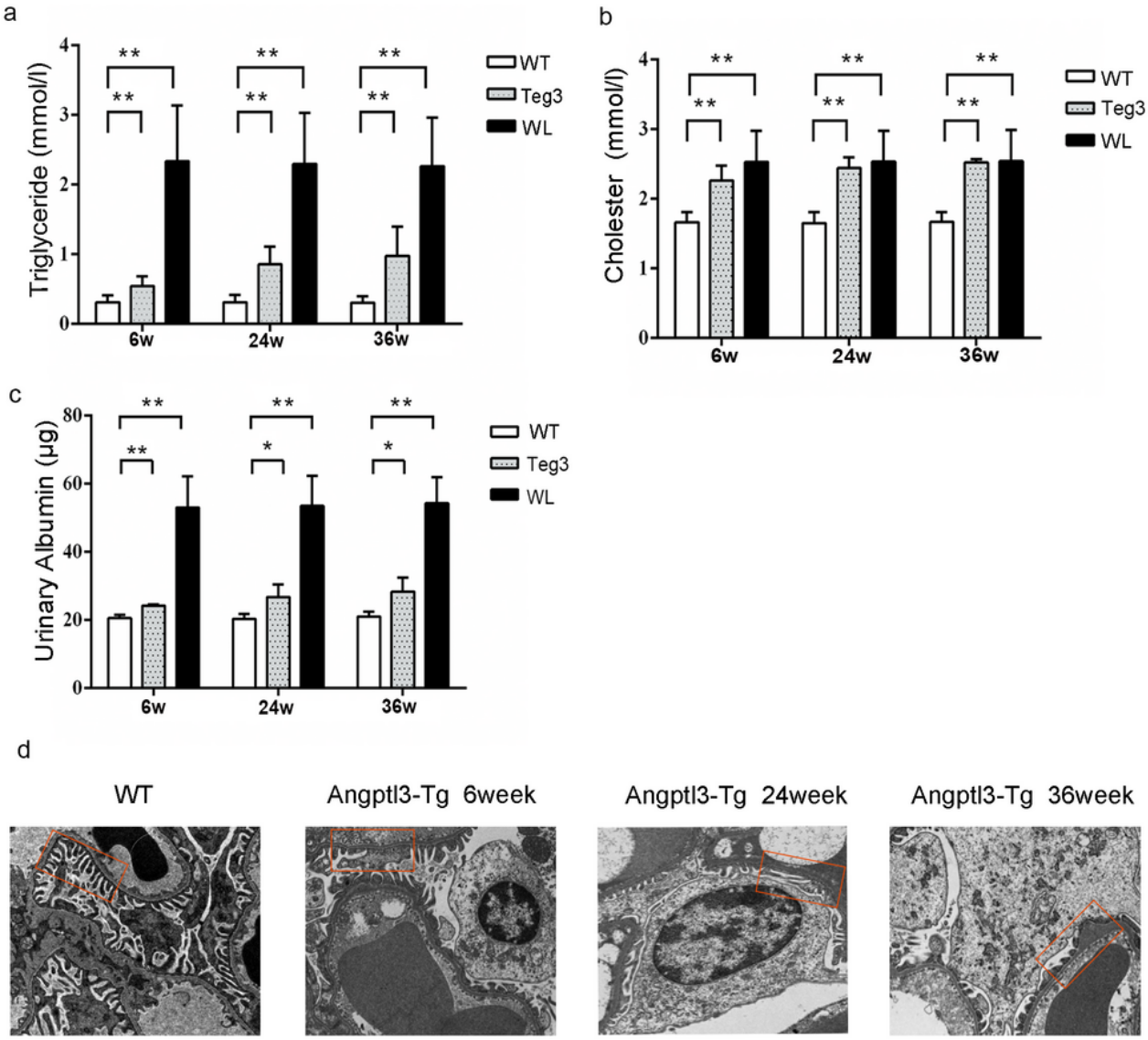

Figure 3

Angptl3-tg mice developed hyperlipidemia and varying degrees of proteinuria. a: Triglyceride levels in angptl3-tg mice were markedly increased at different time points. b: The cholesterol level in angptl3-tg

mice was also significantly higher than that in wild-type mice at every time point. c: Changes in proteinuria levels in the three groups. d: Random EM photographs of the glomerular basement membrane surrounded by epithelium and endothelium were taken at a magnification of 5,000 X. WT: wild-type mice, WL: wild-type mice with LPS stimulation. Each group included 5 mice. *P<0.05 **P<0.01 the P values were subjected to one-way ANOVA.

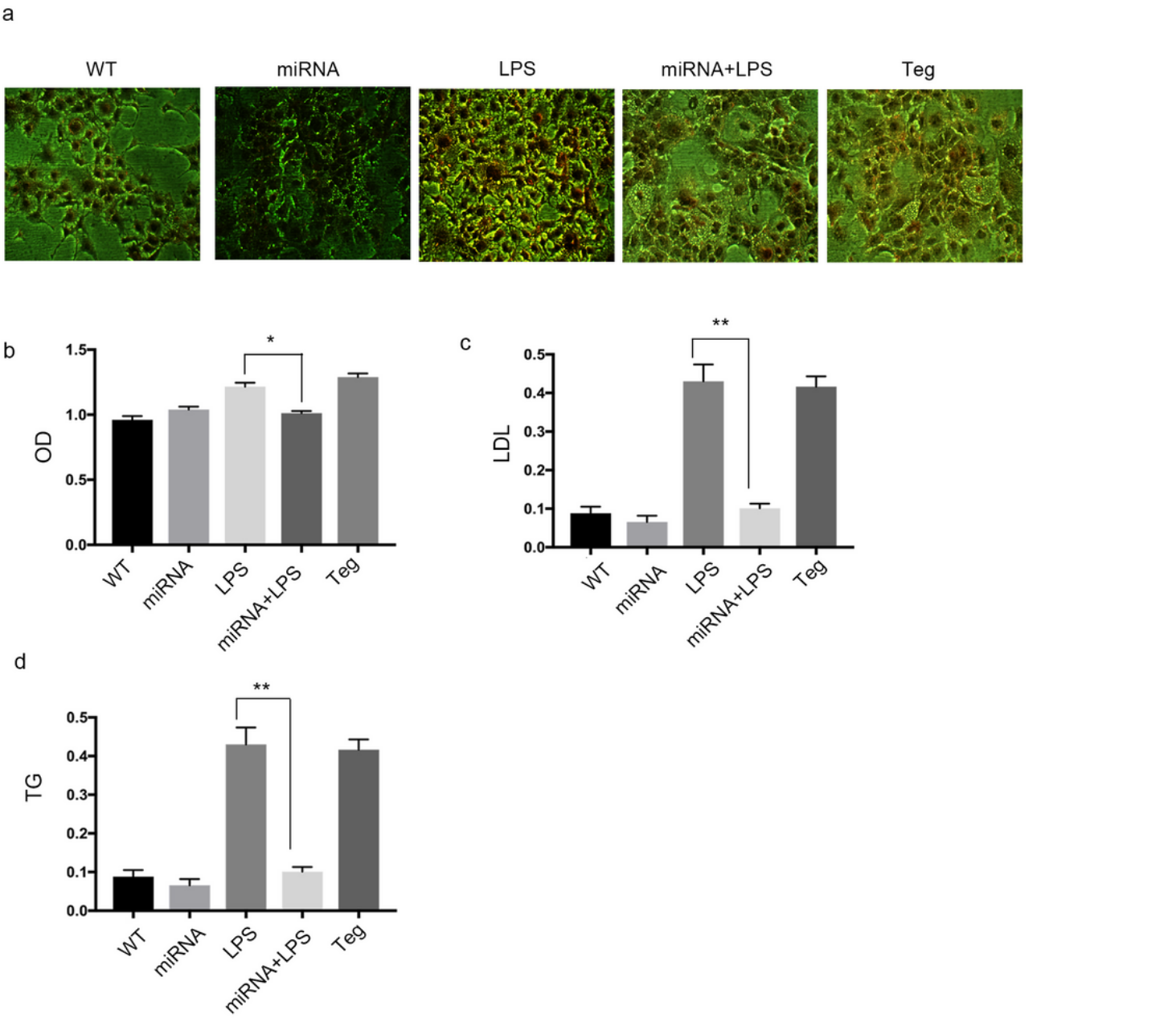

Figure 4

The effects of ANGPTL3 on hepatocytes in the nephrotic state were observed in vitro. a: Red oil staining areas in the different groups, and the magnification is 400 X. b: The OD data from red oil staining. c: ELISA data showing LDL in the different groups. d: Changes in the TG level in the different groups. WT: wild-type hepatocytes, miRNA: angptl3 gene-knockdown hepatocytes, miRNA+LPS: hepatocytes stimulated with LPS after angptl3 knockdown, Teg: hepatocytes transfected with angptl3. Each group included 5 mice. *P<0.05 **P<0.01 the P values were subjected to one-way ANOVA.

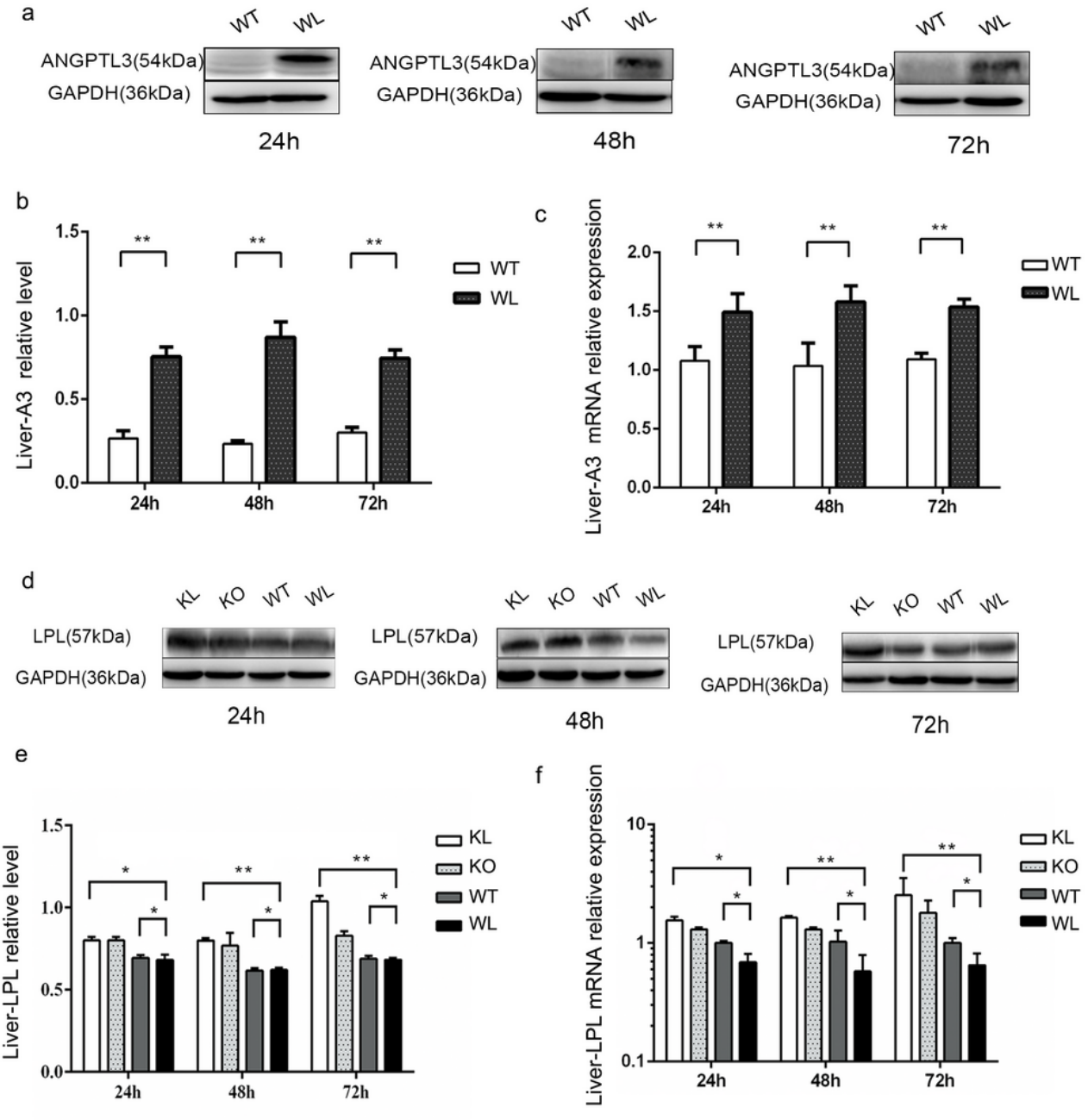

Figure 5

ANGPTL3 may affect the occurrence of PNS hyperlipidemia by impacting LPL expression in mouse liver tissue. a, b, c: The expression of LPL in wild-type or Angptl3-/- mice in physiological and nephritis states. d, e, f: ANGPTL3 expression changes in wild-type or Angptl3-/- mice in physiological and nephritis states. WT: wild-type mice, WL: wild-type mice stimulated with LPS, KO: Angptl3-/- mice, KL: Angptl3-/- mice stimulated with LPS. Each group included 5 mice. *P<0.05 **P<0.01 the P values were subjected to one-way ANOVA.

Supplementary Files

This is a list of supplementary files associated with this preprint. Click to download.

- supplement2.tif
- supplement1.tif
- supplementtable.docx